

Gravity or turbulence? II. Evolving column density PDFs in molecular clouds

Javier Ballesteros-Paredes^{1*}, Enrique Vázquez-Semadeni¹, Adriana Gazol¹, Lee W. Hartmann², Fabian Heitsch³, and Pedro Colin¹

¹ *Centro de Radioastronomía y Astrofísica, Universidad Nacional Autónoma de México, Apdo. Postal 72-3 (Xangari), Morelia, Michocán 58089, México*

² *Department of Astronomy, University of Michigan, 500 Church Street, Ann Arbor, MI 48105, USA*

³ *Department of Physics and Astronomy, University of North Carolina Chapel Hill, CB 3255, Phillips Hall, Chapel Hill, NC 27599, USA*

Submitted to MNRAS, 25 September 2018

ABSTRACT

It has been recently shown that molecular clouds do not exhibit a unique shape for the column density probability distribution function (N -PDF). Instead, clouds without star formation seem to possess a lognormal distribution, while clouds with active star formation develop a power-law tail at high column densities. The lognormal behavior of the N -PDF has been interpreted in terms of turbulent motions dominating the dynamics of the clouds, while the power-law behavior occurs when the cloud is dominated by gravity. In the present contribution we use thermally bi-stable numerical simulations of cloud formation and evolution to show that, indeed, these two regimes can be understood in terms of the formation and evolution of molecular clouds: a very narrow lognormal regime appears when the cloud is being assembled. However, as the global gravitational contraction occurs, the initial density fluctuations are enhanced, resulting, first, in a wider lognormal N -PDF, and later, in a power-law N -PDF. We thus suggest that the observed N -PDF of molecular clouds are a manifestation of their global gravitationally contracting state. We also show that, contrary to recent suggestions, the exact value of the power-law slope is not unique, as it depends on the projection in which the cloud is being observed.

Key words: ISM: general – clouds – kinematics and dynamics – turbulence – stars: formation

1 INTRODUCTION

It has been known since the first observations of molecular gas in star-forming clouds that the CO lines exhibit supersonic line widths (Wilson et al. 1970). Goldreich & Kwan (1974) suggested that such supersonic linewidths could be produced by large-scale collapse of the molecular clouds. In contrast, Zuckerman & Evans (1974) dismissed the idea of large-scale collapse with the argument that, if clouds were collapsing freely, the star formation rate in the Galaxy

should be a factor of 100 times larger than observed, leading to quick exhaustion of its gas content. Those authors proposed instead that the large linewidths are produced by small-scale supersonic turbulence¹.

Since then, the scenario of supersonic molecular cloud turbulence has received much attention, and turbulent models of molecular clouds have been developed by several groups (see Mac Low & Klessen 2004;

¹ Strictly speaking, Zuckerman & Evans (1974) ruled out only *radial* large-scale collapse, which is hardly surprising, as molecular clouds are generally far from round.

* e-mail: j.ballesteros@crya.unam.mx

Ballesteros-Paredes et al. 2007, and references therein). However, the turbulent picture faces several problems, not the least of which is that supersonic shocks dissipate energy quickly, within one dynamical time scale, even if turbulence is magnetized (Stone, Ostriker, & Gammie 1998; Mac Low et al 1998; Padoan & Nordlund 1999). Moreover, although stellar energy has been proposed as a source of turbulence within molecular clouds, it is not clear that such feedback can maintain the identity of the clouds; high-mass stars can easily blow apart clouds, and bipolar flows from low-mass stars are so focused that general support seems unlikely (see review by Vázquez-Semadeni 2010a). Thus it is far from clear - and it has not been demonstrated numerically - that stellar feedback can keep clouds near equilibrium for several dynamical timescales. In fact, the available evidence suggest the opposite (see Vázquez-Semadeni et al. 2010).

The idea that molecular clouds (MCs) are the result of large-scale compressions of the H I diffuse medium was explored with numerical simulations of a 1 kpc squared piece of the galactic disk, representative of the Solar Neighborhood by Ballesteros-Paredes, Vázquez-Semadeni & Scalo (1999) and Ballesteros-Paredes, Hartmann & Vázquez-Semadeni (1999), and collected in a coherent scenario by Hartmann, Ballesteros-Paredes & Bergin (2001). These authors found that MCs can be formed rapidly and proceed to star formation almost at the same time, since the column density threshold for gravitational instability and for molecular gas formation are similar². Simultaneously, Hennebelle & Pérault (1999) discussed the idea of large-scale compressions of the diffuse medium undergoing thermal instability, thus producing dense gas. This led to the idea that molecular clouds in the solar neighborhood are formed in large scale compressions from the warm, diffuse, thermally unstable medium (Heitsch et al. 2006; Vázquez-Semadeni et al. 2007; Heitsch & Hartmann 2008). As these clouds accumulate mass and cool rapidly, they become Jeans unstable; at this point, gravity begins to dominate the motions, developing near equipartition between the gravitational and kinetic energies (Vázquez-Semadeni et al. 2007; Heitsch & Hartmann 2008), erroneously but frequently inferred to be in “Virial Equilibrium” (Ballesteros-Paredes 2006). As a consequence, the initial turbulent fluctuations in density and velocity produce hierarchical fragmentation, in which dense clumps with short free-fall times proceed to a rapid collapse, while at the same time the whole cloud contracts at a slower rate, because of its lower average density.

This model of molecular cloud formation has been subject to different observational tests. For instance, Heitsch et al. (2009) showed that the CO(1-0) observed line profiles through such modeled clouds reproduce the supersonic, turbulent line profiles of actual molecular clouds,

² Note, however, that the entire evolutionary sequence that culminates with the formation of a giant molecular cloud involves timescales of a few tens of Myr, of which the “molecular stage” may represent a small final fraction (Hartmann, Ballesteros-Paredes & Bergin 2001; Bergin et al. 2004; Vázquez-Semadeni et al. 2007, 2010)

as well as the so-called core-to-core velocity dispersion. In other words, such global collapse of irregular structures develops internal disordered, turbulent motions at some level, and thus the large linewidths in actual MCs must be showing mainly the large-scale systematic, inhomogeneous inward motions, rather than pure turbulence. In fact, Vázquez-Semadeni et al. (2009) showed that the culmination of the collapse of a medium-sized cloud produces a dense clump with large velocity dispersion, with physical properties similar to those of massive star-forming regions. In this clump, the velocity field is dominated by the collapse motions.

In addition, Ballesteros-Paredes et al. (2011), based on observations of massive dense cores (Caselli & Myers 1995; Plume et al. 1997; Shirley et al. 2003; Gibson et al. 2009; Wu et al. 2010), showed that the Larson (1981) relationship between velocity dispersion and size arises naturally if turbulent motions are the result of hierarchical and chaotic global + local collapse. In particular, they found that the velocity dispersion should scale as

$$\delta v^2 \simeq 2G\Sigma R \quad (1)$$

where δv is the velocity dispersion of the gas, Σ is the column density of the core, R its size, and G the universal constant of gravity, according to the Heyer et al. (2009) relation recently found for molecular clouds.

In the present work we take a further step to compare models with observations. We analyze the column density probability distribution function from models of molecular cloud formation and evolution via warm, thermally unstable H I stream collision. The goal of the present contribution is to assess the evolution of the column density probability distribution function (N -PDF) in these models, and compare it to the N -PDF of observed molecular clouds. This is particularly important because a number of recent observations have reported N -PDF for several nearby molecular clouds, permitting more tests of theory.

In section §2 we discuss the current knowledge of volumetric and column density pdfs for interstellar gas. In §3.1 we briefly describe the models used, and in §3 we present the time evolution of our N -PDFs. In §4 we present a brief discussion and in §5 we give our main conclusions.

2 VOLUMETRIC AND COLUMN DENSITY PDFS OF MOLECULAR CLOUDS

One important tool for understanding the internal structure of molecular clouds is the volume density probability distribution (ρ -PDF). For isothermal, turbulent flows of a given Mach number M , where shocks occur stochastically and in succession, creating density fluctuations $\rho_1/\rho_0 \propto M^2$, the ρ -PDF is a lognormal function, i.e., a Gaussian function in the logarithm of the density. Vázquez-Semadeni (1994) and Passot & Vázquez-Semadeni (1998) explain this result as follows: in an isothermal flow, the speed of sound is spatially uniform, and a shock of intensity M will induce a density jump ρ_1/ρ_0 over the mean density ρ_0 . If another shock of intensity M arrives at the place where the density is now ρ_1 , it

will induce another density jump of size $\rho_2/\rho_1 \propto M^2$. Thus, if the flow is stochastic, such density jumps must be spatially uniform, and a given density distribution must be obtained by a succession of multiplicative density jumps, which are additive in the logarithm. Thus, at a given position in space, each density jump is independent of the previous and the following ones, and therefore, the central limit theorem, according to which the distribution of the sum of identically-distributed, independent events approaches a Gaussian, can be applied to the logarithm of the density, resulting in a lognormal density probability distribution function.

Various authors suggested that the column density of turbulent, isothermal flows must also be lognormal (e.g., Ostriker et al. 2001; Ridge et al. 2006). However, this is only a consequence of the fact that interstellar turbulence contains the largest velocities at the largest scales, and thus, the size of the interstellar clouds is comparable to their correlation length. In this case, Vázquez-Semadeni & García (2001) showed that the local values of the volume density along a single line of sight are correlated, and thus the column density might be representative of the mean value of the volume density along such line of sight. Thus, for different lines of sight, the values of the N -PDF are correlated to the mean values of the ρ -PDF, and thus, the N -PDF follows the shape of the ρ -PDF. This would not be the case, however, if the correlation lengths of molecular clouds were small. In this case, the line of sight will contain many correlation lengths, and thus, the mean value will not be representative of the volumetric density of the line of sight. In this case, the central limit applies over the sum of several correlation lengths, and the column density should exhibit a Gaussian shape (Vázquez-Semadeni & García 2001).

In recent years, a number of observational studies have focused on understanding the column density PDF of nearby clouds. For instance, Ridge et al. (2006) used extinction data from the COMPLETE (COordinated Molecular Probe Line Extinction Thermal Emission) Survey of Star-Forming Regions, to argue that the gas in Ophiuchus and Perseus molecular clouds exhibits a lognormal N -PDF (see also Goodman et al. 2009). Unfortunately, the column density in this work is plotted in linear scale in the y axis (number of events), and thus, the excess in the high column density part of the N -PDF cannot be properly appreciated. However, that excess clearly indicates that some degree of departure of the lognormality is going on in Perseus.

On the other hand, Froebrich et al. (2007) presented maps and N -PDFs of 14 different regions inferred from extinction measurements. They found that the N -PDFs exhibit different shapes, although the dynamical range in visual extinction A_V is frequently smaller than one order of magnitude, making it difficult to draw firm conclusions about the actual shape of the N -PDF for these clouds.

Kainulainen et al. (2009) took this a step further, showing that the Coalsack and Lupus V molecular clouds, which do not have signs of star formation, exhibit lognormal N -PDFs, while clouds that have already formed stars, like Taurus and Lupus I, do exhibit power-law like tails at large column densities. Their results were confirmed almost immediately afterwards by Froebrich & Rowles (2010). The

standard interpretation of both groups is that clouds that are turbulent and non-star forming, exhibit a lognormal N -PDF, while clouds that are forming stars are somehow decoupled, and exhibit a power-law tail at large column densities.

The above observational results have a clear counterpart in numerical simulations of star formation in turbulent, isothermal MCs. Several groups have shown that the ρ -PDFs in those simulations develop power-law tails at late stages (Klessen 2000; Dib & Burkert 2005; Vázquez-Semadeni et al. 2008). More recently, Kritsuk et al. (2010) have shown that centrally-peaked density distributions, such as the singular isothermal sphere Shu (1977), or other dynamical solutions such as a pressure-free or inside-out collapse, which are all characterized by power-law density profiles, have ρ -PDFs and N -PDFs with power-law high-density tails, whose slope does in fact depend on the slope of the density profile. Also, they show that numerical simulations of self-gravitating isothermal turbulence develop power-law tails as time progresses. Thus, they attribute the development of such tails in self-gravitating turbulent flows to the formation of local collapsing sites. Although they do not mention it explicitly, one can conjecture that the PDFs of the entire turbulent flow exhibit the characteristic power-law tails of the collapsing centers, because the latter are the only sites where such high densities develop. Note also that, because those authors only evolved their simulations to less than half a free-fall time, the dominant component of the kinetic energy in the simulations was still that due to the turbulent flow.

On the other hand, multiphase simulations of the formation and evolution of MCs out of the convergence of warm, diffuse gas in the presence of self-gravity by Vázquez-Semadeni et al. (2007, 2010) and Heitsch & Hartmann (2008) show that the dominant component of the kinetic energy in the clouds after they become dominated by self-gravity is generalized gravitational contraction. In the remainder of this paper, we show that those multiphase simulations also develop power-law tails in their N -PDFs at late times, suggesting that the PDFs of MCs should not be expected to be stationary, but rather to evolve in time, as a consequence of the transition of the clouds from being turbulence dominated to being collapse dominated.

As an alternative interpretation, Tassis et al. (2010) have recently shown that a lognormal column density PDF does not necessarily imply that the flow is turbulent. In particular, they have shown that simulations of individual and multiple collapses also exhibit lognormal N -PDFs at early stages in their evolution. However, it is well known that isothermal compressible turbulence develops such a lognormal PDF Vázquez-Semadeni (1994); Passot & Vázquez-Semadeni (1998). Thus, it is natural to ascribe the lognormal parts of PDFs of ISM turbulence simulations to supersonic isothermal turbulence. Similarly, the high-density gas in the ISM is characterized by supersonic linewidths and behaves very close to isothermally, suggesting that lognormal PDFs in MCs are due to this process as well.

In the next section we will show that this behavior can

be understood in a unified model of molecular cloud formation and evolution, where clouds are assembled by large-scale convergent flows in the WNM, which initially produce turbulence, but gravity rapidly takes over, producing a hierarchy of nested collapsing motions, and thus, the N -PDF develops a power-law wing at large column densities.

3 RESULTS

3.1 Brief description of the models

In the present section we analyze the evolution of the N -PDF in numerical simulations of the formation and evolution of molecular clouds. In order to understand the evolution of the N -PDF, we briefly describe the evolution of the clouds of those simulations (for a review, see Vázquez-Semadeni 2010b).

The models consist in the collision of two large streams of warm thermally bi-stable H I gas. The streams collide with a given inflow velocity, on top of which fluctuations in magnitude and shape are superposed.

As the streams collide, the compressed regions undergo a nonlinearly induced thermal instability, cooling down rapidly and becoming turbulent due to a combination of various instabilities (Heitsch et al. 2005, 2006; Vázquez-Semadeni et al. 2006). As the cold clouds accumulate mass, they quickly become Jeans unstable at various scales. The superposition of those different centers of collapse produces hierarchy of nested collapses, which is reflected in highly supersonic line profiles (Heitsch et al. 2009; Ballesteros-Paredes et al. 2011) that traditionally have been interpreted as evidence of turbulence.

Under this general scheme, several studies (e.g., Vázquez-Semadeni et al. 2007; Heitsch & Hartmann 2008; Vázquez-Semadeni et al. 2010) have performed simulations with different numerical schemes (SPH, fixed grid or AMR, respectively), and with slightly different initial conditions. However, in spite of the differences, the formation and evolution of the modeled molecular clouds exhibit similar characteristics: initially, all modeled clouds fragment rapidly due to dynamical and thermal instabilities, as well as the initial velocity fluctuations. However, while the models without gravity remain fragmented and do not develop large density regions, the models with gravity start to collapse transversely to the inflow direction, developing local centers of collapse with large volumetric densities ($\geq 10^6 \text{ cm}^{-3}$), as well as large column densities, ($\geq 10^{24} \text{ cm}^{-2}$).

As Heitsch & Hartmann (2008) discuss, the same cloud at different evolutionary times appears as if it were different kind of objects: at earlier times, the compressed layer could be classified as a diffuse H I cloud, with low column densities and thus, very little CO content (see Heitsch et al. 2006; Vázquez-Semadeni et al. 2006). As time goes by, the layer accumulates more mass, column densities increase, and some CO begins to form. At this stage the cloud could be identified as a “translucent” cloud. Later in time, larger column densities are achieved not only because of the compression of gas along the direction of the streams, but because

the transverse collapse causes a rapid increase of the column density, shielding the interior of the cloud against UV photons. At this stage, the cloud appears mostly molecular, with dense cores that are already collapsing and which a few Myr later form stars. The precise times in which each one of these stages occurs depends on several parameters, e.g., the initial values of the density and velocity fields, the actual values of their fluctuations, the total mass of the streams, etc. However, once the cloud has accumulated enough mass to allow for molecule formation, the first collapsed objects appear a few Myr later.

In the present work, in order to focus on the shape of the N -PDF during the process of cloud formation, we make use of runs without stellar feedback. We use runs HF and GF2 of the suite presented by Heitsch & Hartmann (2008) and LAF0 run by Vázquez-Semadeni et al. (2010). Run HF is similar to GF2, but without self-gravity, and is used only for reference. Run GF2 represents the evolution of a $\sim 22 \times 44 \times 44$ pc cube filled with gas at $T \sim 1800$ K and at a density of $n = 3 \text{ cm}^{-3}$. The incoming streams are ellipsoidal cylinders with a cross section of 22 pc, an inflow velocity of 7.9 km/sec, and inflow boundary conditions on the numerical box, i.e., infinite incoming cylinders. In run LAF0, the simulation is performed using an adaptive mesh refinement numerical scheme (ART code by Kravtsov et al. 1997). The box has a size of 256 pc per side, filled with a gas at $T = 5000$ K, and a density of $n = 1 \text{ cm}^{-3}$. The streams are circular cylinders having a diameter of 32 pc, and an incoming velocity of 5.9 km/sec, and a length of 110 pc. The inflows are thus fully contained within the box. This means not only that they have a finite length and duration, but also that the total mass of the box in the Vázquez-Semadeni et al. (2010) runs is constant, while in the runs by Heitsch & Hartmann (2008) it is not. This result will have implications on the height of the N -PDF, as we will see in §3.2.

In order to trigger instabilities in the compressed layer, in the HF and GF2 runs the shock front has a sinusoidal shape, while in LAF0 run, a fluctuating velocity field is added to the inflow velocity with rms amplitude of $\sim 30\%$ of the inflow speed, and with $\sim 1/2$ the diameter of the inflows. For more details, see conditions of runs GF2 and LAF0 for Heitsch & Hartmann (2008) and Vázquez-Semadeni et al. (2010), respectively.

3.2 Column density PDFs

Figs. 1, 2, and 3 show the N -PDFs of models HF, GF2 and LAF0, respectively. For each run, we present two extreme cases: N -PDFs calculated by projecting the density field perpendicular to the inflow and one projecting along it. All plots exhibit 16 panels, from 3 to 15 Myr in Figs. 1 and 2, and from 5.6 Myr to 26.6 Myr in Fig. 3. In both cases, the time is measured from the beginning of the collision. The first point to notice in all three figures is that in all the simulations, at every time step, and in both projections, there is a large number of data points at low column densities. This is just a consequence of the setup of the simulations: the incoming flows are cylindrical, and outside these cylinders

the gas is uniform, with low volume density and zero initial velocity. The peaks in each case simply reflect the column density of the uniform background medium. The mean density of this field is $\sim 1 \text{ cm}^{-3}$, and thus, the typical column density of this part of the box is $\sim 2 \times 10^{20} \text{ cm}^{-2}$ for run GF2 and $\sim 8 \times 10^{20} \text{ cm}^{-2}$ for the LAF0 one.

The second point to notice is that the column densities in both projections are extreme cases because these are extreme projections. Typically, molecular clouds must be observed at intermediate angles. In any case, the initial N -PDFs for the projection along the flow (plane $y-z$) are narrower than the projections perpendicular to the flow (planes $x-y$ or $x-z$, not showed here). This is because the clouds are formed in the $y-z$ plane, and hence the cloud is thinnest along the x -direction.

In all three figures we further show lognormal and/or power-law fits as follows: Fig. 1 shows only lognormal fits (dotted line) at every timestep, since the corresponding run is purely hydrodynamical. Note that the PDF increases in height as time goes on. This is a consequence of the inflow boundary conditions of the models from Heitsch & Hartmann (2008), which imply that the total mass in the box increases in time.

In Figs. 2 and 3, on the other hand, we show the lognormal fits from $t = 5.3 \text{ Myr}$ to $t = 9.1 \text{ Myr}$ and from $t = 9.8 \text{ Myr}$ to $t = 16.8 \text{ Myr}$, respectively. The final times of these intervals correspond to the time at which the cloud start collapsing more vigorously. However, for reference, we keep the first fit until the end of the simulation (dot-dashed line).

We note that in both panels of Fig. 1 the N -PDFs exhibit a lognormal-like wing at large column densities (dotted line) since early on in the simulation's evolution, and maintain this shape for the rest of the evolution. The lognormal wing at large column densities is due to the density fluctuations produced by the turbulence induced by a combination of nonlinear thin shell, thermal and Kelvin-Helmholtz instabilities in the compressed layer (Heitsch et al. 2005). However, it is worth noting that this lognormal part is quite narrow, with column densities spanning less than two orders of magnitude, from $\sim 2 \times 10^{21} \text{ cm}^{-2}$ to 10^{23} cm^{-2} , for the entire duration of the evolution. This is due to the fact that the turbulence generated by the instabilities is not very strong, in agreement with previous results (Koyama & Inutsuka 2002).

The case with self-gravity is quite different (see Figs. 2 and 3). We divide the behavior in two cases: the lognormal and the power-law behaviors. We first note that, after some transients, the dense column density region develops a narrow lognormal shape, indicated by the dotted line (which we maintain through all frames for clarity). However, as time goes on, gravity modifies the lognormal shape, first by making it wider. In order to show this widening more clearly, in Fig.4 we plot the evolution of the standard deviation σ of the lognormal fits as a function of time for the four runs with self-gravity. From this figure it is clear that the lognormals tend to increase in width as the collapse proceeds. This behavior has been recently reported by Tassis et al. (2010). Finally, at late times, gravity runs away and column density grows several orders of magnitude in a few Myr. As a

consequence, the N -PDF develops a power-law tail at large column densities.

The N -PDFs shown in Figs. 2 and 3 are reminiscent of the variety of N -PDFs for different clouds shown by Kainulainen et al. (2011). In fact, as shown by Froebrich et al. (2007), every cloud may have its own slope, depending not only on the physical conditions of the cloud, but also on the resolution at which the cloud itself has been observed.

Furthermore, by comparing the direction of the projections, we note that the slope depends on the orientation of the cloud: although in models GF2 the slope in both projections is almost the same (see Fig 2), models LAF0 (Fig 3) show that the slope is steeper when we observe the cloud along its longer dimension. This effect occurs because if the cloud is mostly aligned with the line of sight, the observed column densities will be larger than the column densities obtained if the cloud is mostly on the plane of the sky. This result contrasts with the suggestion by Kritsuk et al. (2010) that all the N -PDFs should tend to evolve towards a single value. These authors used a model of a spherical cloud, and thus every projection is the same. However, real clouds are far from round, and thus one cannot expect an asymptotic single value of the slope of the power-law tail of the N -PDF.

Also, it is noteworthy that the other run with slightly different perturbations in Heitsch & Hartmann (2008), (run GF1, not shown), which has a smaller perturbation in the shock front, has an N -PDF evolution which is basically indistinguishable from the one presented here for model GF2. Similarly, the run with smaller amplitude fluctuations (SAF0, also not shown) in Vázquez-Semadeni et al. (2010), follows an N -PDF evolution indistinguishable from model LAF0. However, the precise time in which each model (Heitsch & Hartmann 2008; Vázquez-Semadeni et al. 2010) start collapsing are different: $t \sim 10 \text{ Myr}$ for the Heitsch & Hartmann (2008) runs, and $t \sim 15 \text{ Myr}$ for the Vázquez-Semadeni et al. (2010) runs. The difference seems to be due to the free-fall time in each run: the compressed region in the Heitsch & Hartmann (2008) runs has 47% of the volume of the compressed region in Vázquez-Semadeni et al. (2010), but its mass flux is 5 times larger. Thus, the density in the compressed region is 2.23 times larger in the Heitsch & Hartmann (2008) run, which in turn implies a free-fall timescale $2/3$ times smaller. This result suggests that, to first order, the main parameters that define the time of collapse are the velocity and the density of the incoming field. Indeed, a parameter study by Rosas-Guevara et al. (2010) has found widely different star formation efficiencies and times of the onset of star formation as parameters such as the inflow velocity and the amplitude of the background turbulent fluctuations are varied.

In both runs, after the development of the lognormal N -PDF, a clear power-law tail develops at high column densities. This shape transition marks also the beginning of the accelerated large-scale collapse ongoing simultaneously with the small-scale local collapses, and occurs in few Myr ($\sim 4 - 5 \text{ Myr}$), regardless of the particular setup of the runs. It seems thus that once the cloud has achieved enough shielding to form molecules, the cloud proceeds to

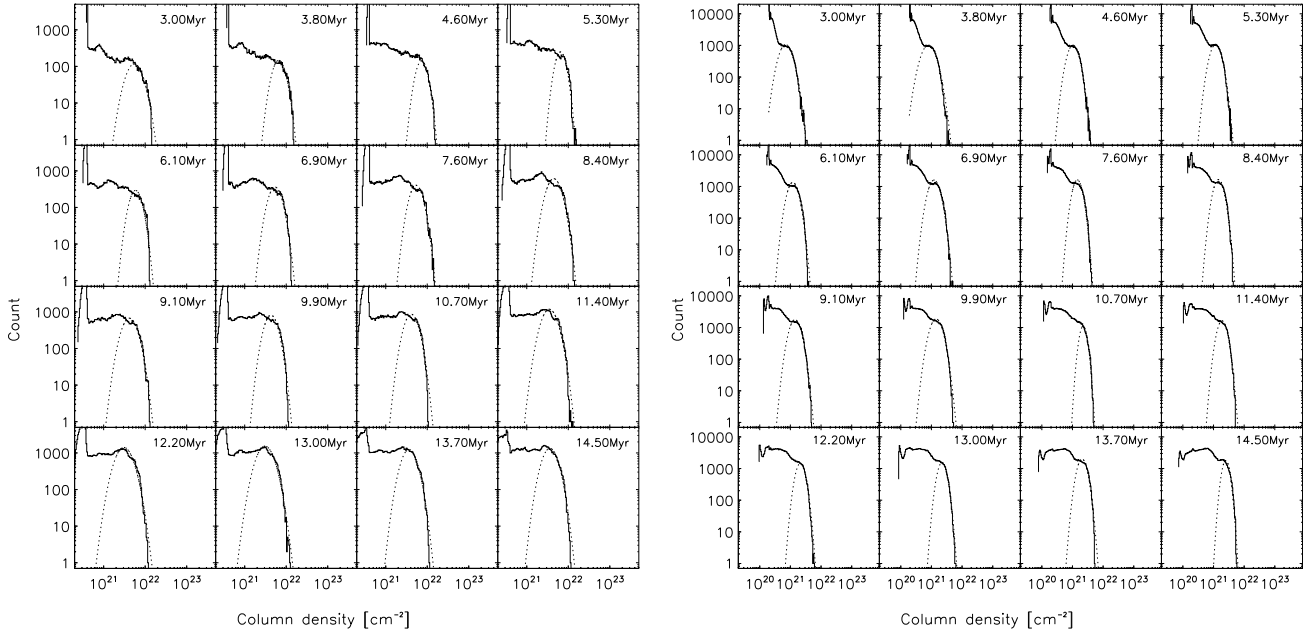


Figure 1. a) Time evolution of the column density probability distribution function of a run without self-gravity (run HF in Heitsch & Hartmann 2008) seen perpendicular to the flow (edge on). b) Same as a), but for the projection along the flow (face on).

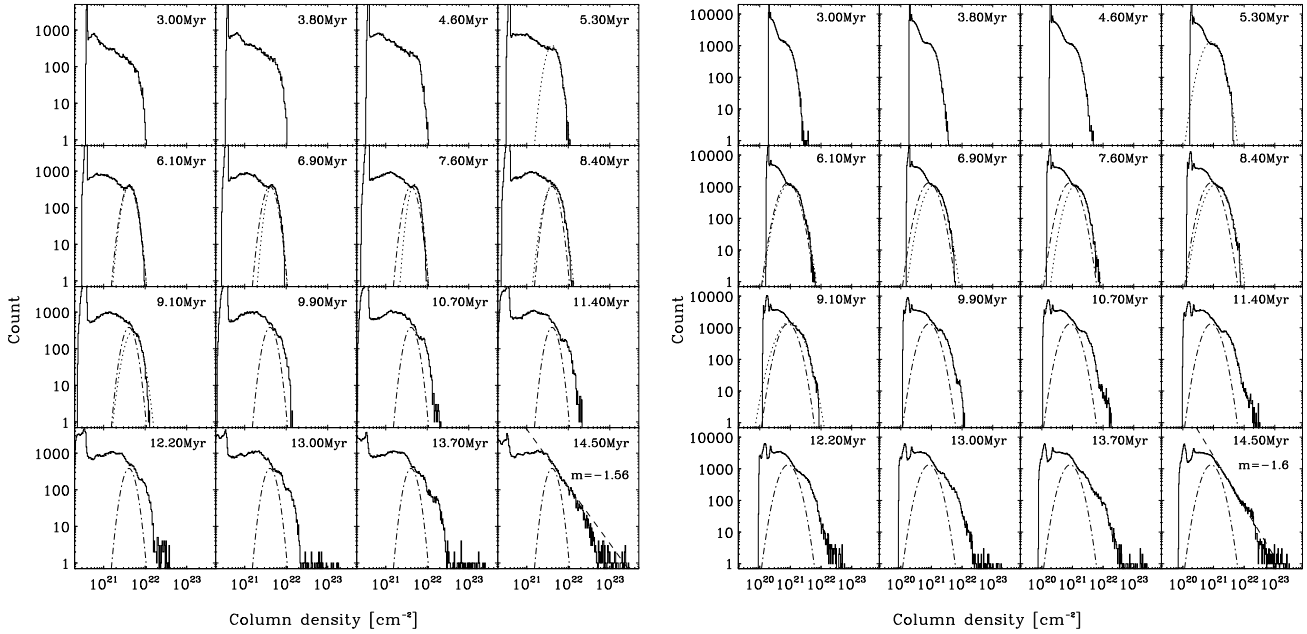


Figure 2. a) Time evolution of the column density probability distribution function of a run including self-gravity (run GF2 in Heitsch & Hartmann 2008) seen perpendicular to the flow (edge on). b) Same as a), but for the projection along the flow (face on).

collapse in few Myr, as pointed out by Heitsch & Hartmann (2008). The rapidity of this transition explains why most of the molecular clouds in the Solar Neighborhood exhibit young star forming regions (few Myrs), and there are only

few clouds with no signs of star formation (Coalsack, Lupus V, see Kainulainen et al. 2009).

Thus, we conclude that as global+local collapses proceed, the number of high column density points in the N -PDFs increases, causing a high N -

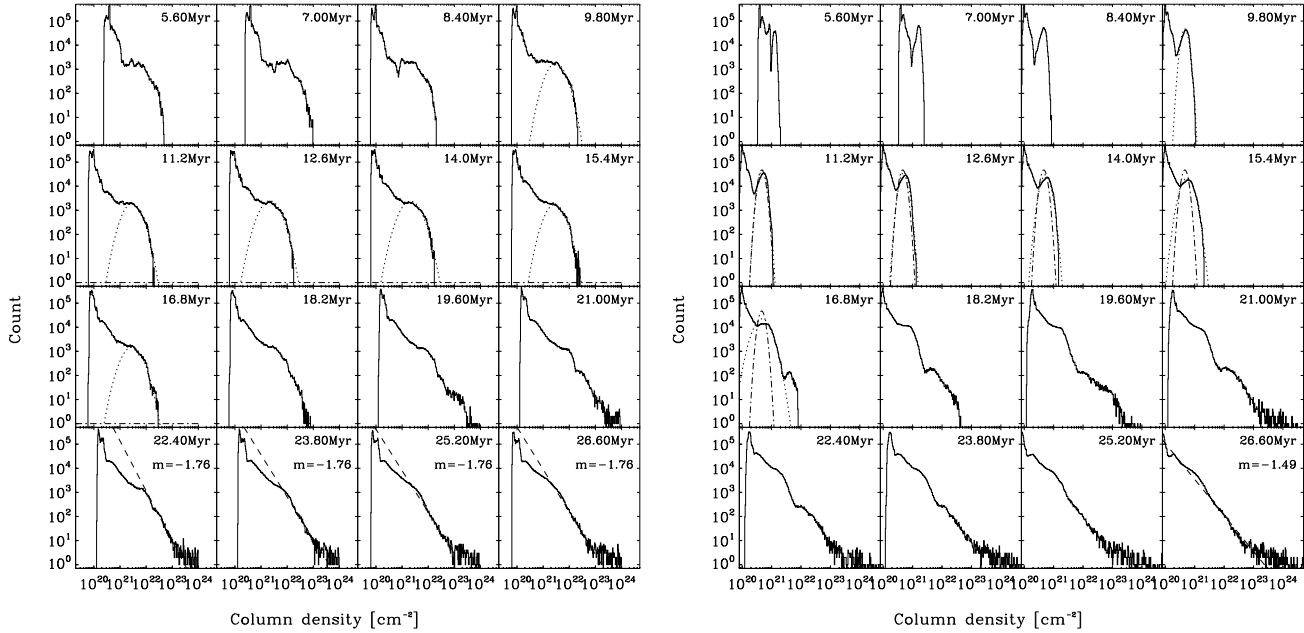


Figure 3. a) Time evolution of the column density probability distribution function of model LAF0 in Vázquez-Semadeni et al. (2010) seen perpendicular to the flow (edge on). b) Same as a), but for the projection along the flow (face on).

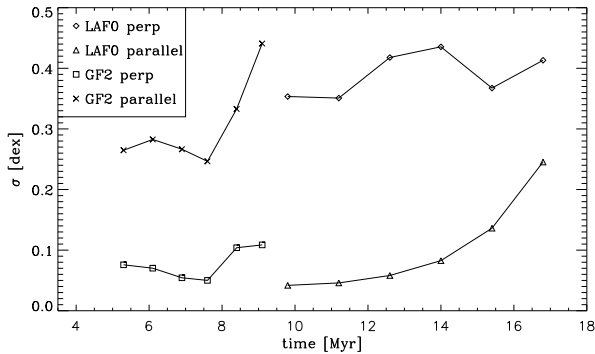


Figure 4. Time evolution of the standard deviation of the lognormal function fitted in the two projections of the two runs with self-gravity. As can be seen, in all cases σ increases with time, implying that gravity makes wider the lognormal of a purely turbulent gas.

PDF tail. As pointed out by Franco & Cox (1986); Hartmann, Ballesteros-Paredes & Bergin (2001) and Heitsch & Hartmann (2008), in the Solar Neighborhood the pressure due to self-gravity becomes important at about the column density necessary to shield the compressed region against UV radiation (10^{21} cm^{-2}), allowing the formation of molecules. This situation corresponds to the 3rd row in the rightmost column of Fig. 1 in Heitsch & Hartmann (2008), and corresponds to the moment in which the cloud has already started to collapse in the direction perpendicular to the shock. At this moment, the densest cores of the cloud reach column densities of 10^{23} cm^{-2} .

4 DISCUSSION

Froebrich et al. (2007), Kainulainen et al. (2009) and Froebrich & Rowles (2010), argue that the different shapes of the observed N -PDFs must be due to a change in the governing physical processes in molecular clouds. In particular, Froebrich & Rowles (2010) argue that most of their N -PDFs can be fitted by a lognormal distribution, plus a power-law wing, the first one for low column densities, which corresponds to the gas that is not forming stars, and the second one for the gas which is forming stars.

Our results show that these two regimes (quiescent vs. active star formation) may very well be part of a single evolutionary process, as depicted by Kainulainen et al. (2009). In the early stages of the molecular cloud, the H I colliding streams form the molecular gas and provide part of the supersonic turbulent kinetic energy observed in the line profiles. During this stage, the N -PDF is lognormal, and most of this stage occurs in the atomic phase (Vázquez-Semadeni et al. 2007; Heitsch & Hartmann 2008), during which the cloud does not form stars. Later on, hierarchical and chaotic gravitational contraction takes over, tending to produce a power-law tail in the N -PDFs. The initial manifestation of this effect is that the lognormal appears to become wider. It is important to mention that gravity is required in order to achieve the 1.5–2 orders of magnitude in the spread of the column density values, since pure turbulence produces only very narrow lognormal N -PDFs. The contribution of self-gravity in increasing the column density helps the cloud to achieve values high enough to rapidly form molecular gas, as pointed out by Heitsch & Hartmann (2008); Heitsch et al. (2009). A few Myr after the molecules

have formed, the densest cores collapse and the first stars begin to form.

Although we agree with the general scheme depicted by Kainulainen et al. (2009), we stress that the contribution of self-gravity is indispensable to achieve high values of the column density. That is, self-gravity is not only important in driving the collapse of gravitationally unstable clumps, but also in *forming* such clumps, which would not be produced by turbulence alone (Vázquez-Semadeni et al. 2008). During the later stages, the primary source of “turbulent” motions (i.e., supersonic linewidths) in the molecular cloud is gravity as well, with local mass concentrations that render the velocity field more locally complex (Heitsch et al. 2009; Ballesteros-Paredes et al. 2011).

5 CONCLUSIONS

Using numerical models of the formation and evolution of molecular cloud from the diffuse interstellar medium, we have confirmed the suggestion by Kainulainen et al. (2009) that the N -PDF transits from a lognormal shape at early times, when the kinetic energy in the clouds is dominated by their initial turbulence (produced by various instabilities in the compressed layer that becomes the cloud), to having a power-law tail at high N at late times, when their kinetic energy is dominated by gravitational contraction, which culminates with the formation of stars. Our results thus explain naturally recent observations showing that non-star-forming clouds exhibit lognormal N -PDFs, while star-forming clouds exhibit power-law tails at high densities, understanding the result as the consequence of the transition of the clouds from a more diffuse, turbulence-dominated regime to a denser, star-forming, collapsing one. We also have shown that the slope of the power-law tail produced by gravity in the N -PDF does not have a unique value, but depends on the orientation of the cloud with respect to the line of sight.

ACKNOWLEDGEMENTS

This work has received partial support from grants UNAM/DGAPA IN110409 to JBP, CONACYT 102488 to EVS, NSF AST-0807305 to LH and FH, and has made extensive use of the NASA’s Astrophysics Data System Abstract Service.

REFERENCES

- Ballesteros-Paredes J. J. 2006 MNRAS, 372, 443
 Ballesteros-Paredes, J., Hartmann, L. W., Vázquez-Semadeni, E., Heitsch, F., & Zamora-Avilés, M. A. 2011, MNRAS, 411, 65
 Ballesteros-Paredes, J., Hartmann, L. & Vázquez-Semadeni, E. 1999, ApJ, 527, 285
 Ballesteros-Paredes, J., Vázquez-Semadeni, E., & Scalo, J. 1999, ApJ, 515, 286
 Ballesteros-Paredes, J., Klessen, R. S., Mac Low, M.-M., Vázquez-Semadeni, E. 2006, in Protostars and Planets V, eds. B. Reipurth, D. Jewitt, K. Keil (Tucson: Univ. of Arizona Press), in press (astro-ph/0603357)
 Bergin, E. A., Hartmann, L. W., Raymond, J. C., & Ballesteros-Paredes, J. 2004, ApJ, 612, 921
 Caselli, P., & Myers, P. C. 1995, ApJ, 446, 665
 Dib, S., & Burkert, A. 2005, ApJ, 630, 238
 Franco, J., & Cox, D. P. 1986, PASP, 98, 1076
 Froebrich D., Murphy G. C., Smith M. D., Walsh J., Del Burgo C. 2007. MNRAS 378, 1447
 Froebrich D., Rowles J. MNRAS, submitted (2010arXiv1004.0117F)
 Gibson, D., Plume, R., Bergin, E., Ragan, S., & Evans, N. 2009, ApJ, 705, 123
 Goldreich, P. & Kwan, J. 1974, ApJ 189, 441
 Goodman, A. A., Pineda, J. E., & Schnee, S. L. 2009, ApJ, 692, 91
 Hartmann, L., Ballesteros-Paredes, J., & Bergin, E. A. 2001, ApJ, 562, 852
 Heitsch, F., Ballesteros-Paredes, J., & Hartmann, L. 2009, ApJ, 704, 1735
 Heitsch, F., Burkert, A., Hartmann, L. W., Slyz, A. D., & Devriendt, J. E. G. 2005, ApJL, 633, L113
 Heitsch, F., & Hartmann, L. 2008, ApJ, 689, 290
 Heitsch, F., Slyz, A. D., Devriendt, J. E. G., Hartmann, L. W., & Burkert, A. 2006, ApJ, 648, 1052
 Hennebelle P., Pérault M. 1999. A&A, 351, 309
 Heyer, M., Krawczyk, C., Duval, J., & Jackson, J. M. 2009, ApJ, 699, 1092
 Kainulainen, J., Beuther, H., Banerjee, R., Federrath, C., & Henning, T. 2011, arXiv:1104.0678
 Kainulainen, J., Beuther, H., Henning, T., & Plume, R. 2009, A&A, 508, L35
 Klessen, R. S., 2000, ApJ, 535, 869
 Koyama, H. & Inutsuka, S.-I. 2002, ApJ, 564, L97
 Kravtsov, A. V., Klypin, A. A., & Khokhlov, A. M. 1997, ApJS, 111, 73
 Kritsuk, A. G., Norman, M. L., & Wagner, R. 2010, arXiv:1007.2950
 Larson, R. B. 1981, MNRAS, 194, 809
 Mac Low, M.-M., & Klessen, R. S. 2004, Reviews of Modern Physics, 76, 125
 Mac Low, M.-M., Klessen, R. S., Burkert, A., & Smith, M. D. 1998, Phys. Rev. Lett., 80, 275
 Ostriker, E. C., Stone, J. M., & Gammie, C. F. 2001, ApJ, 546, 980
 Padoan, P. & Nordlund, Åke 1999, ApJ, 526, 279
 Passot T., Vázquez-Semadeni, E. 1998, Phys. Rev. E 58, 4501
 Plume, R., Jaffe, D. T., Evans, N. J., II, Martin-Pintado, J., & Gomez-Gonzalez, J. 1997, ApJ, 476, 730
 Ridge, N. A., et al. 2006, AJ, 131, 2921
 Shirley, Y. L., Evans, N. J., II, Young, K. E., Knez, C., & Jaffe, D. T. 2003, ApJS, 149, 375
 Rosas-Guevara, Y., Vázquez-Semadeni, E., Gómez, G. C., & Jappsen, A.-K. 2010, MNRAS, 406, 1875
 Shu, F. H. 1977, ApJ, 214, 488
 Stone, J. M., Ostriker, E. C., & Gammie, C. F. 1998, ApJL,

- 508, L99
- Tassis, K., Christie, D. A., Urban, A., Pineda, J. L., Mouschovias, T. C., Yorke, H. W., & Martel, H. 2010, MNRAS, 408, 1089
- Vázquez-Semadeni E. 1994. ApJ423, 681
- Vázquez-Semadeni, E. 2010, arXiv:1010.5157
- Vázquez-Semadeni, E. 2010, arXiv:1009.3962
- Vázquez-Semadeni, E., Colín, P., Gómez, G. C., Ballesteros-Paredes, J., & Watson, A. W. 2010, ApJ, 715, 1302
- Vázquez-Semadeni E., García N. 2001. ApJ 557, 727
- Vázquez-Semadeni, E., Gómez, G. C., Jappsen, A. K., Ballesteros-Paredes, J., González, R. F., & Klessen, R. S. 2007, ApJ, 657, 870
- Vázquez-Semadeni, E., Gómez, G. C., Jappsen, A.-K., Ballesteros-Paredes, J., & Klessen, R. S. 2009, ApJ, 707, 1023
- Vázquez-Semadeni, E., González, R. F., Ballesteros-Paredes, J., Gazol, A., & Kim, J. 2008, MNRAS, 390, 769
- Vázquez-Semadeni, E., Ryu, D., Passot, T., González, R. F., & Gazol, A. 2006, ApJ, 643, 245
- Wilson, R. W., Jefferts, K. B., & Penzias, A. A. 1970, ApJL, 161, L43
- Wu, J., Evans, N. J., Shirley, Y. L., & Knez, C. 2010, ApJS, 188, 313
- Zuckerman, B., & Evans, N. J., II 1974, ApJL, 192, L149